Quantifying Reliability and Resilience in Interdependent Infrastructure Networks

Risat Rimi Chowdhury[1], Om Prakash Yadav[2], Maneesh Singh[3], and Shah M Limon[4]

[1,2]*North Carolina A&T State University, Greensboro, North Carolina, 27411, USA*
rchowdhury@aggies.ncat.edu
oyadav@ncat.edu

[3]*Western Norway University of Applied Sciences, Inndalsveien 28, Bergen, Norway*
Maneesh.Singh@hvl.no

[4]*Slippery Rock University, Slippery Rock, Pennsylvania, 16075, USA*
shah.limon@sru.edu

ABSTRACT

Infrastructure networks such as power, water, and communication systems are interdependent, and disruptions in one network can propagate across others, causing performance loss and delayed recovery. Although prior studies have modeled recovery and evaluated resilience in such systems, few have examined their operational limits through reliability analysis. This study develops a simulation-based framework to quantify reliability and resilience in two partially interdependent networks while considering node failure and recovery. The critical percolation threshold is identified from the cascading failure process and used in a voting system model to compute system reliability. Results show that higher coupling strength shifts the percolation threshold to a larger value and reduces system reliability, whereas lower coupling strength allows the system to sustain connectivity under a greater degree of node failure. Resilience is evaluated through a cascading recovery process following complete disruption of one network. Recovery of a node enables restoration of its dependent counterpart in the other network, propagating sequentially across both networks. Multiple simulation scenarios are employed to represent uncertainty in the node recovery process. Results indicate that higher coupling strength leads to greater initial disruption in the dependent network but facilitates faster and more coordinated recovery in both networks. Thus, reliability and resilience exhibit opposing trends with coupling strength. An interdependency index is also introduced to support management decisions for interdependent infrastructure networks. This framework provides a structured basis for understanding how inter-network connectivity affects system reliability and recovery dynamics.

1. INTRODUCTION

Infrastructure networks are interconnected, and this interdependence enhances everyday convenience but also introduces the risk of cascading failures (CFs) (Buldyrev, Parshani, Paul, Stanley, and Havlin, 2010). CFs often extend beyond the initially affected network and can quickly propagate to interdependent networks (Xiao, Zhao, Wu, Chen, Gong, Zhu, and Liu, 2022). Although interdependency among infrastructure networks has existed for a long time, increasing interconnectedness across global systems creates the potential for more severe consequences. For instance, the M9.0 Tohoku-Oki earthquake in Japan (2011) (Kobayashi, 2014) and the M7.4 Central Sulawesi earthquake in Indonesia (2018) (Paulik, Gusman, Williams, Pratama, Lin, Prawirabhakti, Sulendra, Zachari, Fortuna, Layuk, & Suwarni, 2019) caused widespread failures across interdependent infrastructure networks.

Accurate reliability assessment is essential for maintaining the optimal performance of interdependent critical infrastructure (CI) networks. Overlooking interdependency can substantially overestimate network performance (Miao, Liu, Zhong, Han, Hou, & Du, 2025). Terminal reliability has been extensively applied in interdependent networks and is defined as the probability of establishing connectivity between source and terminal nodes (Wilkov, 2003). Commonly used algorithms for terminal reliability computation include the state enumeration method (Shier, 1991), the sum of disjoint products method (Wilson, 2002), the minimal cuts method (Chowdhury, Yadav, & Limon, 2024), and cellular automata (Zio, Podofillini, & Zille, 2006). However, terminal reliability analysis does not explicitly consider a network's operational limits (Zio, 2009), which focus on identifying the minimum fraction of functional components required to sustain the network. Percolation theory addresses this limitation by examining the critical point at which the failure of a proportion of network

components leads to network failure (Cohen & Havlin, 2010). This point is known as the percolation threshold and serves as a statistical measure of the network's operational limits (Li, Zhang, Zio, Havlin, & Kang, 2015). The threshold also provides a basis for evaluating system reliability (Elsayed, 2012).

With growing interdependence among CI networks, researchers have emphasized the need to understand resilience under failure propagation (Satumtira & Dueñas-Osorio, 2010; Bešinović, 2020; Lu et al., 2024). Network flow models (Holden, Val, Burkhard, & Nodwell, 2013), agent-based simulations (Barton, Eidson, Schoenwald, Stamber, & Reinert, 2000), system dynamics approaches (Zhang, Han, Meng, & Wang, 2012), probabilistic graphical models (Applegate & Tien, 2019), topological vulnerability methods (Li, Lin, Li, Wang, Zhang, & Gao, 2020), and optimization-based resilience frameworks (Ghorbani-Renani et al., 2020; Bellè, 2022) have been used to analyze failure propagation in coupled infrastructure networks. These approaches have addressed network optimization (González, Dueñas-Osorio, Sánchez-Silva, & Medaglia, 2016), resilience measurement (Sharma, Tabandeh, & Gardoni, 2020), and integrated recovery frameworks (Iannacone, Sharma, Tabandeh, & Gardoni, 2022). However, reliability assessment and resilience evaluation are often treated separately, and few studies have considered both in analyzing the performance of interdependent networks. This study addresses this gap by evaluating the reliability and resilience of two partially interdependent networks. Reliability is examined using the critical percolation threshold of the CF process and a voting system model. Resilience is evaluated through a cascading recovery simulation in which the recovery of a node in one network triggers the restoration of its dependent counterpart in the other.

2. PROPOSED METHODOLOGY

This section presents a framework for modeling the reliability and resilience of interdependent networks by incorporating CFs and recovery processes into network performance evaluation. A set of infrastructure networks W, indexed by w and l, is considered, where each network w is represented by a node set N^w and a link set E^w. Each network is modeled as an undirected Erdős-Rényi (ER) graph (Erdős & Rényi, 1960). An ER network is a random graph constructed by randomly placing E links among N nodes, forming a statistical ensemble in which all possible configurations are equally probable (Buldyrev et al., 2010). To simplify the analysis, the CF and recovery mechanisms are defined based on node functionality. The following assumptions are made in the analysis:

- Each network is composed of bidirectional links placed in an uncorrelated manner.
- A node in one network depends on at most one node in the other network.

The proposed framework consists of three main stages: (1) modeling partial interdependencies between two networks; (2) estimating system reliability based on the critical percolation threshold of the CF process; and (3) quantifying network resilience by evaluating system performance during recovery across a set of uncertain scenarios.

2.1. Dependencies and Interdependencies

Dependencies and interdependencies connect multiple networks. If a node in network A relies on a node in network B, failure of the node in network B can cause reduced functionality or complete failure of the node in network A. When this dependency exists in both directions, the relationship is termed an interdependency (Setola, 2010). Representing these relationships is challenging because dependencies and interdependencies can take many forms. For instance, power substations require control equipment that operates through the communications network, such as the internet. Power failure can affect communication networks, which can then disrupt additional power stations, creating a cascading effect. Interdependency between two networks is often partial in real-world systems because some nodes depend on nodes in the other network, whereas others operate independently. For example, in communication and power systems, a fraction of servers may be protected by emergency power supplies that activate when the local power station shuts down.

In this study, we consider two partially interdependent ER networks. To represent partial coupling, a fraction q_1 of nodes in Network 1 depends on nodes in Network 2. Similarly, a fraction q_2 of nodes in Network 2 depends on nodes in Network 1. The degree distributions of Network 1 and Network 2 are denoted by $P_1(k)$ and $P_2(k)$, respectively. Interdependencies are established by randomly pairing nodes between the two networks, ensuring that each node is limited to a single inter-network connection.

2.2. Reliability Analysis of Interdependent Networks

We use the percolation threshold of the CF process in interdependent networks as an indicator of network connectivity loss and as a basis for estimating the reliability of the interdependent system. In percolation theory, node/link failure is represented through removal. As the removal process continues, the network transitions from a connected phase to a disconnected phase. More generally, percolation theory is used to determine the level of node/link failure at which the entire network breaks down. This theory is based on the clustering behavior of networks (Gaur, Yadav, Soni, & Rathore, 2021). It identifies the presence of a threshold probability, p_c, below which the network consists only of isolated clusters that cannot communicate with one another (Albert & Barabási, 2002).

2.2.1. Reliability Estimation

In this study, we analyze how CF triggered by node removal affects the connectivity of interdependent networks. The interdependent network reliability, $R_s(T)$, is assessed using the critical point of the percolation process. Since node percolation and link percolation show similar characteristics (Stauffer & Aharony, 2018), this study focuses solely on node percolation. The process is initiated by randomly removing a fraction 1-p of nodes from one network. If a removed node has a dependent node in the other network, that dependent node is removed as well. Nodes connected to the corresponding network's giant component/cluster through the removed nodes are also considered inactive. As this process continues, the interdependent system fragments into many finite clusters. The system undergoes a percolation transition at the critical threshold, $p = p_c$, and a mutually connected giant cluster exists only when p remains above this threshold. Below this threshold, the entire system becomes completely fragmented (Buldyrev et al., 2010).

In this study, a removed node is considered failed or nonfunctional. Let $R_N(T)$ denote node reliability, defined as the probability that a node remains functional at time T. For an interdependent network with N nodes, the critical point p_c of the percolation process is identified to establish the condition under which the interdependent network collapses. When the fraction of removed or failed nodes, 1-p, i.e., 1-$R_N(T)$ is small, only small clusters break away from the mutual giant cluster where $p_c < R_N(T) < 1$. As the number of removed/failed nodes increases and $R_N(T)$ approaches p_c, the size of the fragments separating from the main cluster increases. At the critical threshold p_c, the main cluster fragments into small pieces, causing the system to fall apart (Bunde & Havlin, 2012). According to percolation theory, the interdependent network loses connectivity once the number of removed/failed nodes reaches N- $[N*p_c]$. This feature enables the use of a voting system model (Elsayed, 2012) with threshold ($[N*p_c] + 1$) to assess the reliability of the interdependent network. The voting system aggregates the probabilities of scenarios where the minimum number of functional nodes exceeds $[N*p_c]$, which represents the minimum number of functional nodes required to maintain interdependent network connectivity. Thus, the reliability of the interdependent network at time T can be obtained using a voting system based on the percolation threshold (D. Li et al., 2015):

$$R_s(T) = \sum_{i=\lfloor N*p_c \rfloor+1}^{N} C_N^i \, R_N(T)^i (1 - R_N(T))^{N-i} \qquad (1)$$

Here, C_N^i is the binomial coefficient and $R_N(T)$ is the node reliability, assumed to be same for all nodes. It is additionally assumed that the node lifetime follows an exponential distribution, $R_N(T) = e^{-\lambda T}$, where λ is the scale parameter. Accordingly, the interdependent network reliability becomes:

$$R_s(T) = \sum_{i=\lfloor N*p_c \rfloor+1}^{N} C_N^i \, (e^{-\lambda T})^i (1 - (e^{-\lambda T}))^{N-i} \qquad (2)$$

2.3. Resilience Analysis of Interdependent Networks

The resilience measure used in this study reflects network recovery after a disruptive event. The formulation is adopted from (Henry & Emmanuel Ramirez-Marquez, 2012) and applied to multiple networks, as shown in Eq. (3).

$$R_w(T_r|a_l) = \frac{P(T_r|a_l) - P(T_d|a_l)}{P(T_0) - P(T_d|a_l)}, \qquad \forall a_l \in \mathrm{A} \qquad (3)$$

Here, $R_w(T_r)$ denotes the resilience measure of network w evaluated at time T_r, with $R_w(T_r) \geq 0$. T_0 and T_d denote the time of the initial state and the time of the final disruptive state, respectively. $P(T)$ is a performance measure relevant to the network under study. The numerator quantifies the recovery between the point at which the disruption has stabilized and any time $T_r \in (T_d, T_f)$, where T_f denotes the recovery time. The denominator represents the total performance loss. The ratio of these two terms indicates whether the system returns to its original level, recovers only partially, or exceeds its pre-disruption state (Aros-Vera & Thekdi, 2025). $P(T)$ is set to have a minimum value of zero and is bounded above by 100, where $P(T) = 100$ corresponds to full network recovery. Performance can be measured in several ways, including infrastructure quality, the number or percentage of functioning nodes, the size of the largest connected component (giant cluster), or deviation from a benchmark. In this study, performance is measured using the size of the giant cluster.

This study also incorporates risk management concepts into resilience modeling. Let $A = \{a_1, a_2, \dots, a_m\}$ denote the set of uncertain scenarios for which resilience is evaluated. These scenarios represent uncertainty in the recovery process and are modeled by adding nodes to networks step-by-step. To account for variability across scenarios A, $P(T)$ must be calculated as the average, or median, or weighted performance level over a fixed number of scenarios. Scenario selection should depend on the system under study, the needs of decision-makers, and the context of application. Modeling a wide range of meaningful scenarios, rather than a narrow subset, is essential for understanding how different uncertainties affect system behavior.

2.3.1. Interdependency Index

In addition to the resilience measure, this study examines inter-network interaction throughout the recovery process using the interdependency index defined in Eq. (4). The interdependency index D_{wl} is calculated as the correlation coefficient for each pairwise comparison of interdependent networks, with network w defined as $w = 1, \dots, b$ and network l defined as $l = 1, \dots, b$. The term n represents the total number of observations obtained by counting the time steps, modeled as iterations, between the original network disruption and full recovery to the pre-disruption performance level.

$$D_{wl} = \frac{n\sum_{w,l} P_w(T)P_l(T) - (\sum_w P_w(T))(\sum_l P_l(T))}{\sqrt{[n\sum_w P_w(T)^2 - (\sum_w P_w(T))^2]*[n\sum_l P_l(T)^2 - (\sum_l P_l(T))^2]}} \quad (4)$$

Decision-makers can use this index to examine how the number or placement of inter-network connections relates to the recovery behavior of interdependent systems. Several decision support issues (DSIs) associated with this index for specific network structures and applications are outlined below.

- DSI #1: Can an intervention on one network create benefits for the networks to which it is connected and, in turn, improve the larger system being studied? If a network structure shows a sufficiently high interdependency index, this may indicate that focusing an intervention on one network can indirectly help another network. However, a high degree of interdependency may also increase the possibility of CFs when a disruption occurs.
- DSI #2: Which networks benefit when new connections are added to adjacent networks? If the interdependency index increases as connections between networks increase, decision-makers may need to study where such new connections should be placed. Conversely, reducing the number of connections may be appropriate if the level of interdependency becomes high enough to increase the risk of CFs in CIs.
- DSI #3: Which uncertainties have the greatest effect? If the interdependency index varies substantially across the studied scenarios, it may be necessary to determine which scenarios matter most and why. This can guide further study toward understanding how particular disruptive events influence system objectives and help focus decision making on system investment.

The DSIs relevant to a particular network, application, or decision-making context may vary depending on the stakeholders and decision-makers involved, the incentives for network owners to coordinate their investments, and whether the network is considered a CI (Aros-Vera & Thekdi, 2025).

3. NUMERICAL EXPERIMENTS

3.1. Interdependent Network Structure

Two partially interdependent ER networks are used to illustrate the proposed framework, representing critical infrastructures such as power and communication systems. Both networks are randomly generated (Figure 1), and each comprises 50 nodes. Both networks have the same average degree, i.e., $\langle k \rangle = 6$. Each pair of nodes is connected with the same probability, $p_{Link} = \frac{\langle k \rangle}{N-1} = 0.1224$, to ensure full connectivity of each network.

A fraction q_1 of nodes in Network 1 depends on nodes in Network 2, and a fraction q_2 of nodes in Network 2 depends on nodes in Network 1. Interdependencies between the two networks are bidirectional. Three coupling scenarios are examined: a weak coupling case with $q_1 = q_2 = q = 0.2$ (10 inter-network connections), a medium coupling case with $q_1 = q_2 = q = 0.5$ (25 inter-network connections), and a strong coupling case with $q_1 = q_2 = q = 0.8$ (40 inter-network connections). Nodes are randomly paired between the two networks, and it is ensured that each node has no more than one inter-network connection. A node is considered functional if it belongs to the giant component of its network. A coupled node remains functional only when both nodes are connected to the giant component of their respective networks.

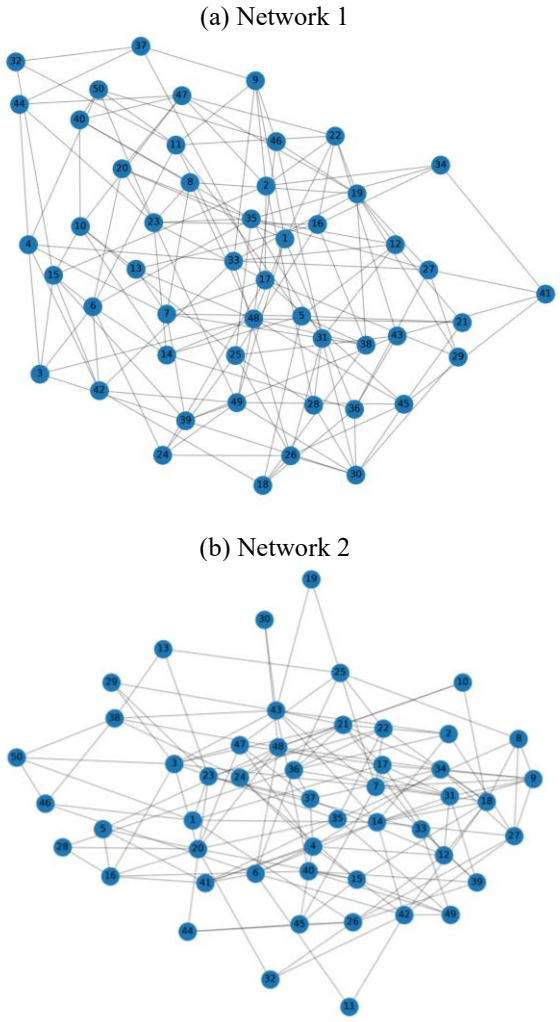

Figure 1. Sample ER networks.

3.2. Partial Interdependent Network Reliability

In this section, the reliability of two partially interdependent ER networks is estimated using the critical point of the percolation process. The percolation properties are studied by randomly removing a fraction $1-p$ of nodes from Network 1, thereby initiating failure. When a node is removed from

Network 1, its links are removed, and any dependent node in Network 2 is also removed. The process then propagates to Network 2, where the giant component is computed, and any nodes disconnected from it are also considered inactive. The same procedure is repeated recursively between the two networks, leading to CFs. This process continues until the system converges either to a mutually connected giant component or to complete fragmentation.

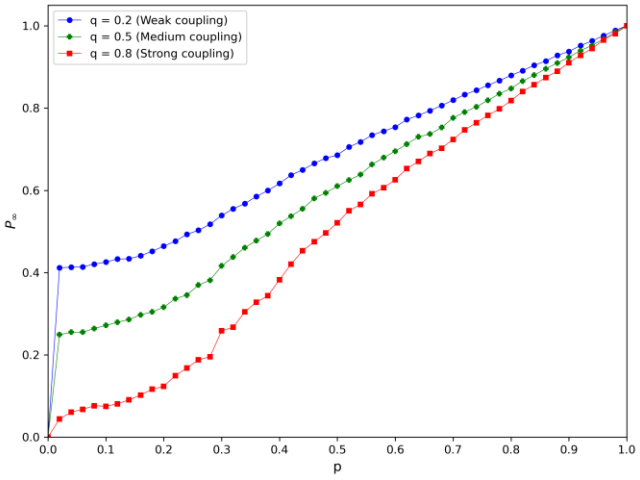

Figure 2. Order parameter $P\infty$ as a function of the fraction of remaining nodes p for two partially interdependent ER networks under weak, medium, and strong coupling.

A percolation transition occurs at a critical threshold p_c, above which a mutually connected giant component exists, and below which the system becomes completely fragmented. Figure 2 shows the fraction of nodes belonging to the mutually connected giant component, $P\infty$, as a function of p for strong (q=0.8), medium (q=0.5), and weak (q=0.2) coupling, based on 50 realizations. A phase-transition behavior is observed across all three coupling scenarios. Under weak and medium coupling, a sharp drop is observed as $P\infty$ approaches zero, whereas under strong coupling, the transition appears less abrupt. This behavior can be attributed to the finite size of the simulated networks and the averaging of results across multiple realizations. The critical threshold is estimated from the P_∞ - p curve using the peak susceptibility criterion, defined as the value of p at which the standard deviation of P_∞ across realizations is maximized (Shu, Wang, Tang, & Do, 2014). Based on this criterion, the estimated thresholds are $p_{c(q=0.2)}$ =0.26, $p_{c(q=0.5)}$ =0.28, and $p_{c(q=0.8)}$ =0.32, with corresponding peak susceptibility values of 0.037, 0.053, and 0.093 for weak, medium, and strong coupling, respectively. (Parshani, Buldyrev, & Havlin, 2010) developed an analytical framework to estimate p_c for interdependent ER networks of large size. For the network settings used in this study, the analytical estimates obtained by numerically solving their generating functions are $p_{c(q=0.2)}$ =0.167, $p_{c(q=0.5)}$ =0.172, and $p_{c(q=0.8)}$ =0.298. The simulated estimates are higher than the analytical predictions, which is expected for small networks with N = 50 nodes. The difference is expected to decrease with increasing network size. The threshold values indicate that higher coupling strength increases vulnerability and shifts the percolation transition to a larger p_c value, thereby reducing the robustness of the coupled system.

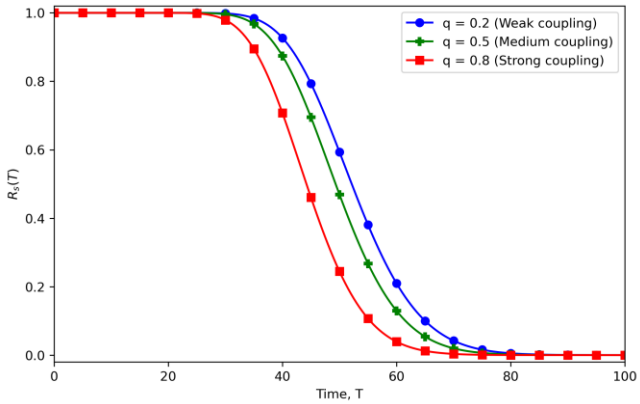

Figure 3. Reliability of interdependent network.

The percolation threshold obtained from the CF process is used as the failure indicator for the partially interdependent network. For the ER networks analyzed in this study, node lifetime is modeled using an exponential distribution, such that $R_N(T)= e^{-\lambda T}$, with λ=0.025. The interdependent network reliability $R_s(T)$ can be obtained from Eq. (2) using the estimated percolation threshold. Figure 3 presents the reliability curves for the three coupling scenarios: strong (q=0.8), medium (q=0.5), and weak (q=0.2). All three curves follow a sigmoidal decline. Under strong coupling, system reliability drops sharply at an earlier time and reaches zero well before the other coupling scenarios. The medium coupling case shows a less abrupt decline, reaching zero earlier than the weak coupling case. The weakly coupled system maintains high reliability over a longer period before gradually declining at a later time. As time increases, nodes begin to fail, and the interdependent network reliability starts to decrease slowly. As more nodes fail and the fraction of functional nodes approaches p_c, the giant component loses connections and more clusters disconnect from it, causing reliability to decrease significantly. This fragmentation occurs sooner for strongly coupled systems since a higher p_c requires a larger fraction of functional nodes to sustain the system, whereas a weakly coupled system tolerates more failures before the giant component fragments completely. Even under medium coupling, the system shows a reduced ability to withstand node failure. This indicates that the interdependent system becomes more vulnerable with increasing coupling strength, which leads to a shorter system lifetime and lower overall reliability. The percolation threshold provides a basis for assessing how many localized failures an infrastructure network can absorb before it loses its ability to operate (Holme, Kim, Yoon, & Han, 2002).

Tracking the current state of the interdependent system relative to p_c therefore provides an indicator of system health, which can inform maintenance decisions before catastrophic failure occurs.

3.3. Resilience Analysis of Partially Interdependent Networks

This section examines the recovery behavior of two partially interdependent ER networks with 10, 25, and 40 inter-network connections, respectively. The model assumes complete failure of all nodes in Network 1 as the initial condition. A node in Network 1 is randomly selected for recovery. Upon recovery of a node in Network 1, its dependent node in Network 2 is recovered in the subsequent time step. The recovered nodes in Network 2 then enable recovery of the corresponding unrecovered dependent nodes in Network 1. This sequential process is characterized as cascading recovery. The process continues until all nodes in both networks are fully recovered. A total of 50 scenarios are considered, with connections assigned randomly. In this study, $P(T)$ is measured as the number of nodes connected to the giant component of their own network. When a node is not connected to the giant component, it is considered non-functional. A dependent node becomes functional when its corresponding dependent node in the other network has also been recovered. Node recovery can occur through three mechanisms: (1) a random node is selected for recovery; (2) a connected supporting node in the other network has been recovered; or (3) a connected supporting node in the same network has been recovered (Aros-Vera & Thekdi, 2025).

Figure 4 shows the recovery behavior of both networks following a major catastrophic failure. Each plot presents the number of functional nodes on the y-axis against time on the x-axis. Each plot starts at time $T = 0$, representing the time at which Network 1 is completely destroyed and begins its recovery process. The results show that recovery behavior depends strongly on the number of inter-network connections. For the 10-connection case, Network 2 retains a considerably higher number of functional nodes at T=0 due to the limited number of dependency links and reaches full recovery earlier than Network 1. For the 25-connection case, the gap between the two networks' recovery trajectories visibly narrows, and both networks reach full recovery in fewer time steps compared to the 10-connection case. For the 40-connection case, despite a more severe initial disruption to Network 2, both networks exhibit a faster and more closely aligned recovery trajectory, reaching full restoration in the fewest time steps among all three cases. This behavior suggests that stronger coupling promotes a more rapid and coordinated cascading recovery process, as recovered nodes trigger recovery within the same network and in the other network.

(a) 10 connections

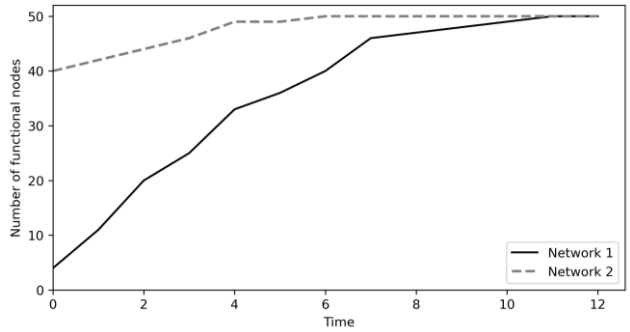

(b) 25 connections

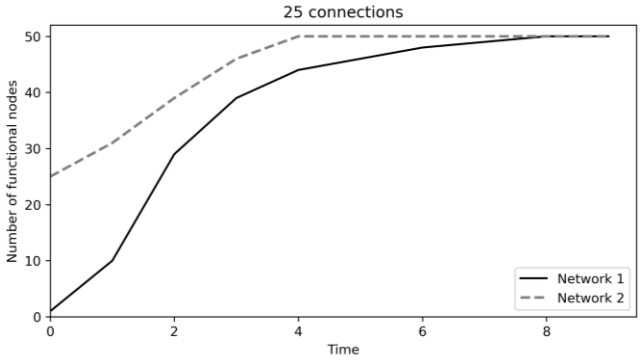

(c) 40 connections

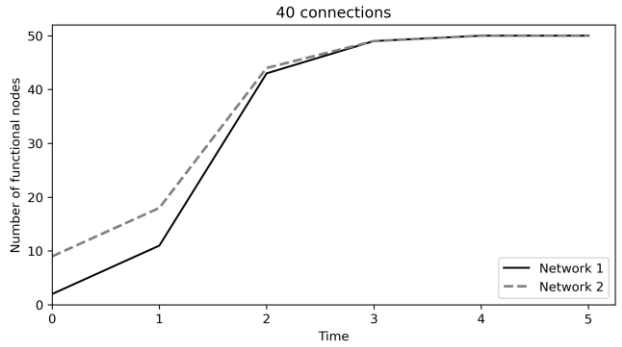

Figure 4. Recovery behavior of interdependent networks.

Figure 5 presents resilience curves of both networks computed using Eq. (3). Across all three coupling scenarios, Network 1 and Network 2 exhibit similar overall recovery behavior. In the 10-connection case, the resilience curves for both networks rise gradually and remain closely aligned over the recovery period. They reach full resilience at the latest time steps among all three cases. As the number of connections increases, both networks recover faster, with the 40-connection case showing both networks reaching full resilience in the fewest time steps. The findings suggest that Network 2 benefits from increased connections to Network 1 through the cascading recovery mechanism, which accelerates the recovery process in both networks.

(a) 10 connections

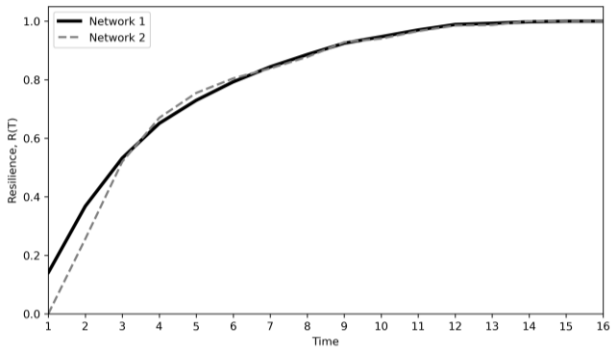

(b) 25 connections

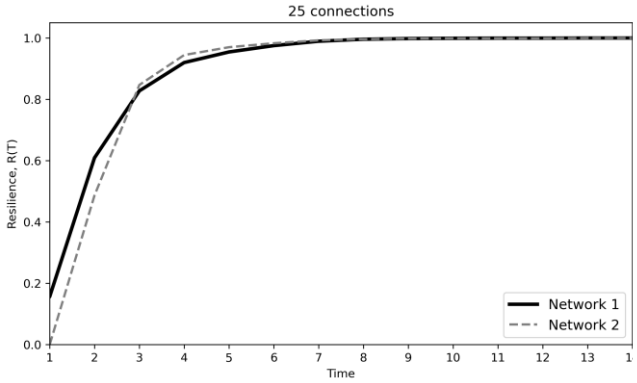

(c) 40 connections

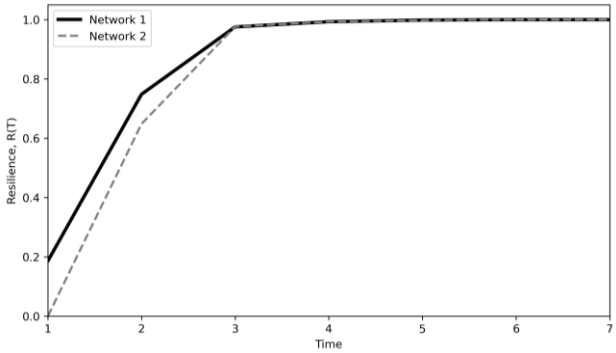

Figure 5. Resilience curves of interdependent networks.

3.4. Interdependency Effect on System Performance

To understand the effect of coupling on interdependent system performance, both the reliability and resilience scores are computed as the normalized areas under their respective curves. Figure 6 presents these scores across the three coupling strengths. The two scores exhibit opposing trends; as coupling strength increases, the reliability score decreases, whereas the resilience score improves. This indicates a trade-off between reliability and resilience with respect to coupling strength.

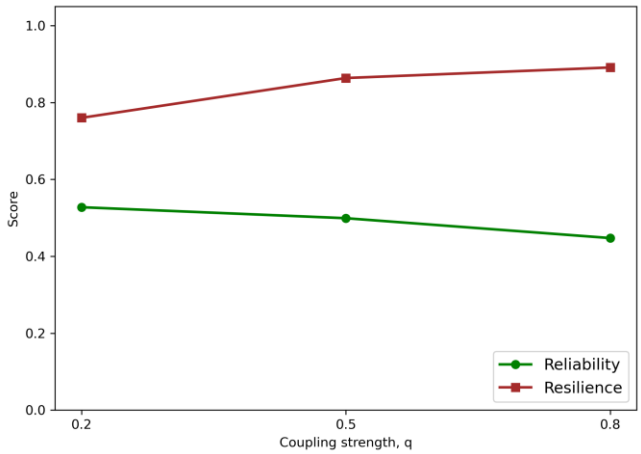

Figure 6. Reliability and resilience scores versus coupling strength, q.

We also examine the interdependency index, D_{wl}, across 50 scenarios for 10, 25, and 40 inter-network connections, as presented in Table 1. All three cases exhibit a high average interdependency index, with values close to 1. The average interdependency index increases as the number of connections increases. Under lower coupling strength, Network 2 is not severely disrupted when Network 1 is destroyed due to the limited number of connections, resulting in a lower average interdependency index. Under higher coupling strength, Network 2 experiences a more severe initial disruption; however, the faster and more coordinated recovery of both networks results in a higher average interdependency index. The decrease in standard deviation with increasing connections also indicates more consistent recovery behavior under higher coupling strength. These results provide insight into the following DSIs:

- DSI #1: For the 25 and 40 connection cases, the average interdependency indices are very close, suggesting that 25 connections may be sufficient to achieve high levels of indirect benefits to connected networks without increasing the number of connections to 40.
- DSI #2: The average interdependency index increases substantially between 10 and 25 connections but exhibits only a marginal increase between 25 and 40 connections, confirming a non-linear relationship between the number of inter-network connections and the interdependency index. If a decision-maker aims to reduce the risk of CFs, critical nodes should be analyzed under a low number of connections. If the goal is to increase the interdependency index, strategically increasing connections toward 25 would yield the highest impact on inter-network recovery coordination.
- DSI #3: In this study, uncertainty arises from the randomly assigned inter-network connections across the simulated scenarios. The 10-connection case shows the highest variability, indicating that weak coupling is more

affected by this uncertainty. Therefore, specific 10-connection scenarios may warrant deeper investigation.

Table 1. Interdependency index.

No. of Connections	Interdependency Index			
	Average	Standard Deviation	Max	Min
10	0.976	0.017	0.995	0.915
25	0.995	0.004	1.000	0.980
40	0.996	0.002	1.000	0.992

4. CONCLUSION

This study develops a simulation-based framework that employs percolation-based reliability estimation and cascading recovery analysis to examine the effects of coupling strength on two partially interdependent ER networks. Each network consists of 50 nodes with the same average degree, and three coupling scenarios are considered: weak, medium, and strong.

The reliability analysis shows that a higher number of inter-network connections shifts the percolation threshold to a larger value, requiring a larger fraction of functional nodes to sustain system connectivity. As a result, interdependent systems with stronger coupling reach zero reliability earlier, whereas weakly coupled interdependent systems maintain higher reliability over a longer period before collapse. In terms of recovery, Network 2 reaches full recovery sooner than Network 1 in the weak-coupling case, as the limited number of dependency links reduces the disruption to Network 2. Under strong coupling, Network 2 experiences greater initial disruption due to a higher number of dependent nodes; however, both networks recover faster and in closer alignment, as a higher number of inter-network connections accelerates cascading recovery across the system. These findings together suggest that coupling strength introduces a trade-off in which higher coupling strength reduces reliability but promotes faster and more coordinated recovery.

The interdependency index is also computed to further characterize recovery coordination between the two networks. The average interdependency index increases as the number of connections increases. The standard deviation declines as well under stronger coupling, indicating more consistent inter-network recovery coordination. The decision support issues structured around this index suggest that increasing connections toward 25 yields the highest impact on inter-network recovery coordination in the studied system. This index thus provides decision-makers with a practical basis for determining the most appropriate coupling level for a given system. The proposed framework will be useful to CI managers in prioritizing coupling investments that aid post-disruption recovery while managing the risk of CFs. However, the current framework is based on finite-size simulations and assumes uniform node reliability for all nodes. It also does not consider link failures, and each node is restricted to binary functionality with at most one inter-network dependency. To address these limitations, future work will account for link failures, multiple dependencies per node, and real-world network topologies, thereby improving the applicability of the framework to more complex interdependent systems.

REFERENCES

Albert, R., & Barabási, A.-L. (2002). Statistical mechanics of complex networks. *Reviews of Modern Physics*, *74*(1), 47.

Applegate, C. J., & Tien, I. (2019). Framework for probabilistic vulnerability analysis of interdependent infrastructure systems. *Journal of Computing in Civil Engineering*, *33*(1), 04018058.

Aros-Vera, F., & Thekdi, S. (2025). Modeling and managing resilience and risk for interdependent networks. *Socio-Economic Planning Sciences*, *97*, 102105. https://doi.org/10.1016/j.seps.2024.102105

Barton, D. C., Eidson, E. D., Schoenwald, D. A., Stamber, K. L., & Reinert, R. (2000). *Aspen-EE: An agent-based model of infrastructure interdependency*. Sandia National Lab.(SNL-NM), Albuquerque, NM (United States); Sandia ….

Becker, R., Casteigts, A., Crescenzi, P., Kodric, B., Raskin, M., Renken, M., & Zamaraev, V. (2026). Giant components in random temporal graphs. *SIAM Journal on Discrete Mathematics*, *40*(2), 449–485.

Bellè, A. (2022). *Resilience and coupling of interdependent critical infrastructures: Models, optimization, and operations*. Université Paris-Saclay.

Bešinović, N. (2020). Resilience in railway transport systems: A literature review and research agenda. *Transport Reviews*, *40*(4), 457–478. https://doi.org/10.1080/01441647.2020.1728419

Buldyrev, S. V., Parshani, R., Paul, G., Stanley, H. E., & Havlin, S. (2010). Catastrophic cascade of failures in interdependent networks. *Nature*, *464*(7291), 1025–1028. https://doi.org/10.1038/nature08932

Bunde, A., & Havlin, S. (2012). *Fractals and disordered systems*. Springer Science & Business Media.

Chowdhury, R. R., Yadav, O. P., & Limon, S. M. (2024). Reliability Analysis of Interdependent Stochastic-Flow Networks. *2024 Annual Reliability and Maintainability Symposium (RAMS)*, 1–6.

Cohen, R., & Havlin, S. (2010). *Complex networks: Structure, robustness and function*. Cambridge university press.

Elsayed, E. A. (2012). *Reliability Engineering* (2nd ed., Vol. 88). John Wiley & Sons.

Erdős, P., & Rényi, A. (1960). On the evolution of random graphs. *Publ. Math. Inst. Hung. Acad. Sci.*, 5:17.

Gaur, V., Yadav, O. P., Soni, G., & Rathore, A. P. S. (2021). A literature review on network reliability analysis and its engineering applications. *Proceedings of the Institution*

of Mechanical Engineers, Part O: Journal of Risk and Reliability, *235*(2), 167–181.

Ghorbani-Renani, N., González, A. D., Barker, K., & Morshedlou, N. (2020). Protection-interdiction-restoration: Tri-level optimization for enhancing interdependent network resilience. *Reliability Engineering & System Safety*, *199*, 106907. https://doi.org/10.1016/j.ress.2020.106907

González, A. D., Dueñas-Osorio, L., Sánchez-Silva, M., & Medaglia, A. L. (2016). The Interdependent Network Design Problem for Optimal Infrastructure System Restoration. *Computer-Aided Civil and Infrastructure Engineering*, *31*(5), 334–350. https://doi.org/10.1111/mice.12171

Henry, D., & Emmanuel Ramirez-Marquez, J. (2012). Generic metrics and quantitative approaches for system resilience as a function of time. *Reliability Engineering & System Safety*, *99*, 114–122. https://doi.org/10.1016/j.ress.2011.09.002

Holden, R., Val, D. V., Burkhard, R., & Nodwell, S. (2013). A network flow model for interdependent infrastructures at the local scale. *Safety Science*, *53*, 51–60.

Holme, P., Kim, B. J., Yoon, C. N., & Han, S. K. (2002). Attack vulnerability of complex networks. *Physical Review E*, *65*(5), 056109.

Iannacone, L., Sharma, N., Tabandeh, A., & Gardoni, P. (2022). Modeling Time-varying Reliability and Resilience of Deteriorating Infrastructure. *Reliability Engineering & System Safety*, *217*, 108074. https://doi.org/10.1016/j.ress.2021.108074

Kobayashi, M. (2014). Experience of infrastructure damage caused by the Great East Japan Earthquake and countermeasures against future disasters. *IEEE Communications Magazine*, *52*(3), 23–29. https://doi.org/10.1109/MCOM.2014.6766080

Li, D., Zhang, Q., Zio, E., Havlin, S., & Kang, R. (2015). Network reliability analysis based on percolation theory. *Reliability Engineering & System Safety*, *142*, 556–562.

Li, Y., Lin, J., Li, G., Wang, C., Zhang, C., & Gao, L. (2020). Vulnerability assessment of community-interdependent infrastructure network based on PSDA. *Journal of Infrastructure Systems*, *26*(2), 04020006.

Lu, Q.-C., Li, J., Xu, P.-C., Zhang, L., & Cui, X. (2024). Modeling cascading failures of urban rail transit network based on passenger spatiotemporal heterogeneity. *Reliability Engineering & System Safety*, *242*, 109726. https://doi.org/10.1016/j.ress.2023.109726

Miao, H., Liu, Y., Zhong, Z., Han, J., Hou, B., & Du, X. (2025). Seismic Reliability Evaluation of Interdependent Water and Power Supply Networks. *Earthquake Engineering and Resilience*, *4*(1), 41–60.

Parshani, R., Buldyrev, S. V., & Havlin, S. (2010). Interdependent Networks: Reducing the Coupling Strength Leads to a Change from a First to Second Order Percolation Transition. *Physical Review Letters*, *105*(4), 048701.

Paulik, R., Gusman, A., Williams, J. H., Pratama, G. M., Lin, S., Prawirabhakti, A., Sulendra, K., Zachari, M. Y., Fortuna, Z. E. D., Layuk, N. B. P., & Suwarni, N. W. I. (2019). Tsunami Hazard and Built Environment Damage Observations from Palu City after the September 28 2018 Sulawesi Earthquake and Tsunami. *Pure and Applied Geophysics*, *176*(8), 3305–3321. https://doi.org/10.1007/s00024-019-02254-9

Satumtira, G., & Dueñas-Osorio, L. (2010). Synthesis of modeling and simulation methods on critical infrastructure interdependencies research. In *Sustainable and resilient critical infrastructure systems: Simulation, modeling, and intelligent engineering* (pp. 1–51). Springer.

Setola, R. (2010). How to measure the degree of interdependencies among critical infrastructures. *International Journal of System of Systems Engineering*, *2*(1), 38. https://doi.org/10.1504/IJSSE.2010.035380

Sharma, N., Tabandeh, A., & Gardoni, P. (2020). Regional resilience analysis: A multiscale approach to optimize the resilience of interdependent infrastructure. *Computer-Aided Civil and Infrastructure Engineering*, *35*(12), 1315–1330. https://doi.org/10.1111/mice.12606

Shier, D. R. (1991). *Network reliability and algebraic structures*. Oxford University Press.

Shu, P., Wang, W., Tang, M., & Do, Y. (2014). Simulated identification of epidemic threshold on finite-size networks. *arXiv Preprint arXiv:1410.0459*.

Stauffer, D., & Aharony, A. (2018). *Introduction to percolation theory*. Taylor & Francis.

Wilkov, R. (2003). Analysis and design of reliable computer networks. *IEEE Transactions on Communications*, *20*(3), 660–678.

Wilson, J. M. (2002). An improved minimizing algorithm for sum of disjoint products (reliability theory). *IEEE Transactions on Reliability*, *39*(1), 42–45.

Xiao, Y., Zhao, X., Wu, Y., Chen, Z., Gong, H., Zhu, L., & Liu, Y. (2022). Seismic resilience assessment of urban interdependent lifeline networks. *Reliability Engineering & System Safety*, *218*, 108164. https://doi.org/10.1016/j.ress.2021.108164

Zhang, C., Han, C., Meng, L., & Wang, Y. (2012). Interdependent Dynamic Model and Repairing Strategy of Electric Power and Water Supply Systems. *Journal of Information Systems Engineering & Management*, *21*, 564–570.

Zio, E. (2009). Reliability engineering: Old problems and new challenges. *Reliability Engineering & System Safety*, *94*(2), 125–141.

Zio, E., Podofillini, L., & Zille, V. (2006). A combination of Monte Carlo simulation and cellular automata for computing the availability of complex network systems. *Reliability Engineering & System Safety*, *91*(2), 181–190.

BIOGRAPHIES

Risat Rimi Chowdhury is a Ph.D. student in Industrial and Systems Engineering at North Carolina A&T State University. Her research interests include reliability modeling and design optimization.

Om Prakash Yadav is a Professor and Chair in the Department of Industrial & Systems Engineering at North Carolina Agricultural and Technical State University. His research interests include reliability modeling and analysis, risk assessment, design optimization and robust design, and manufacturing systems analysis.

Professor Maneesh Singh is Head (Cyber-physical Systems Research Group) at the Western Norway University of Applied Sciences. His primary research areas include asset integrity management, inspection and maintenance planning, and predictive maintenance.

Shah M Limon is an Associate Professor of Industrial & Systems Engineering at Slippery Rock University of Pennsylvania. His research interests include reliability-based design, network reliability optimization, stochastic modeling, and additive manufacturing.

APPENDIX

This section provides a brief description of the key network terms used in this study, including the ER network, giant component, node degree, and average degree.

Definition 1. (Erdös-Rényi (ER) random network). An ER network is a random graph, denoted by $G_{N,p}$, with N nodes, where a link is independently added between each pair of distinct nodes with probability p. As p increases, the network becomes more connected (D. Li et al., 2015; Becker et al., 2026).

Definition 2. (Giant component). The giant component is the largest connected subgraph in a network whose size scales proportionally with the total number of nodes N (Erdős & Rényi, 1960).

Definition 3. (Degree of a node and average degree). The degree of node i, denoted by k_i, is the number of links incident to that node. The average degree, denoted by $\langle k \rangle$, represents the average number of links connected to the nodes in the network and is obtained by dividing the total degree of all nodes by the total number of nodes (D. Li et al., 2015).